



**INSTITUTO POTOSINO DE INVESTIGACIÓN
CIENTÍFICA Y TECNOLÓGICA, A.C.**

POSGRADO EN CIENCIAS APLICADAS

**An extreme wind event over the San Luis Potosi
Valley, Mexico**

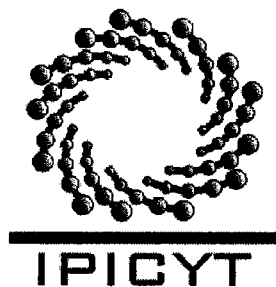
Tesis que presenta
Jorge Gómez Rivera

Para obtener el grado de
Maestro en Ciencias Aplicadas

En la opción de
Ciencias Ambientales

Codirectores de la Tesis:
Dr. José Noel Carbajal Pérez
Dr. Jordi Vila-Guerau de Arellano (Universidad de Wageningen, Holanda)

San Luis Potosí, S.L.P., Octubre de 2004.



Instituto Potosino de Investigación Científica y Tecnológica, A.C.

Acta de Examen de Grado

COPIA CERTIFICADA

El Secretario Académico del Instituto Potosino de Investigación Científica y Tecnológica, A.C., certifica que en el Acta 001 del Libro Primero de Actas de Exámenes de Grado del Programa de Maestría en Ciencias Aplicadas en la opción de Ciencias Ambientales está asentado lo siguiente:

En la ciudad de San Luis Potosí a los 1 días del mes de octubre del año 2004, se reunió a las 12:00 horas en las instalaciones del Instituto Potosino de Investigación Científica y Tecnológica, A.C., el Jurado integrado por:

Dr. José Noel Carbajal Pérez	Presidente	IPICYT
Dr. Alejandro Díaz Ortíz	Secretario	IPICYT
Dr. Alfredo Avila Galarza	Sinodal externo	UASLP

a fin de efectuar el examen, que para obtener el Grado de:

**MAESTRO EN CIENCIAS APLICADAS
EN LA OPCIÓN DE CIENCIAS AMBIENTALES**

sustentó el C.

Jorge Gómez Rivera

sobre la Tesis intitulada:

An extreme wind event over the San Luis Potosi Valley, Mexico

que se desarrolló bajo la dirección de

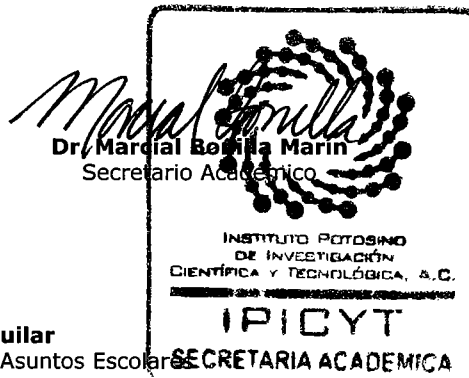
Dr. José Noel Carbajal Pérez
Dr. Jordi Vila-Guerau de Arellano (Universidad de Wageningen, Holanda)

El Jurado, después de deliberar, determinó

APROBARLO

Dándose por terminado el acto a las 14:00 horas, procediendo a la firma del Acta los integrantes del Jurado. Dando fé el Secretario Académico del Instituto.

A petición del interesado y para los fines que al mismo convengan, se extiende el presente documento en la ciudad de San Luis Potosí, S.L.P., México, a los 1 días del mes octubre de 2004.




Mtra. Ma. Elisa Lucio Aguilar
Jefa del Departamento de Asuntos Escolares

to Marcela

The scientist does not study nature because it is useful; he studies it because he delights in it, and he delights in it because it is beautiful. If nature were not beautiful, it would not be worth knowing, and if nature were not worth knowing, life would not be worth living.

Jules Henri Poincaré

Acknowledgments

The author wish to thank, first of all, his parents for their their support without which this Thesis would have never been realized, and secondly Dr. Noel Carbajal Pérez and Dr. Jordi Vila-Guerau de Arellano for their academic support and supervision. Thanks go also to my teachers of IPICYT, especially to Dr. Elisabeth Huber-Sannwald, Dr. Haret Rosu and Dr Tulio Arredondo, all of whom had always some time to give me an advice. Thanks also go to Ing. Adolfo Martínez of the Computer Department of IPICYT for his computational support. Special thanks are for Dr. Alfredo Avila Galarza of Universidad Autonoma de San Luis Potosi for providing the observational data. To M.C. Joaquin Humberto Rodriguez, Director of Meteorologia y Telecoms. Aeronautica for providing observational data and Ing. Modesto Mendoza González from Base de Datos e Imágenes, Servicio Meteorológico Nacional for providing the satellite images.

Contents

1	Introduction	3
2	Study Zone	7
2.1	North of Mexico	7
2.1.1	climate	8
2.1.2	vegetation	8
2.2	The State of San Luis Potosí	9
2.2.1	climate	9
2.2.2	vegetation	10
2.3	The Valley of SLP	11
3	Synoptic Situations	13
4	Methodology	15
4.1	MM5 Model description	16
4.1.1	Governing Equations	16
4.2	Model Configuration	18
4.2.1	Terrain Configuration	18
4.2.2	Boundary Conditions and Vertical Configuration	18
4.2.3	MM5 Configuration and physical options	18
4.3	Observations	19
5	Sensitivity Analysis	21
6	Results and Discussion	23
6.1	Radiation Budget	23
6.2	Turbulent Fluxes	24
6.3	Observations	26
6.3.1	Temperature	26
6.3.2	Wind Speed and Direction	26
6.4	Planetary Boundary Layer	30

6.4.1	Vertical Profiles	30
6.4.2	Stable Boundary Layer	31
6.4.3	Katabatic winds	36
7	Conclusions and future recomendations	39

List of Figures

2.1	<i>North of Mexico Topography</i>	7
2.2	<i>North of Mexico land-use Vegetation Type</i>	8
2.3	<i>San Luis Potosi State Topograhy and principal Elevations(table) and its localization(figure)</i>	9
2.4	<i>State of SLP land-use Vegetation Type</i>	10
3.1	<i>Evolution of the front system over north Mexico on January 23th and 24th of 2004 from satellite infrared data (left side)(source: Servicio Meteorologico Nacional CNA) . Results of the modeled column of water (righth side)</i>	14
4.1	<i>Observational Stations</i>	19
5.1	<i>Sensitivity analyses for two soil moisture values</i>	22
6.1	<i>Surface Radiation Budget Components for two cases: January case(a), and May case(c)</i>	24
6.2	<i>Time evolution of Heat Fluxes and Friction Velocity</i>	25
6.3	<i>Comarison of UST, wind speep and T diference</i>	26
6.4	<i>Dirnual variation of Teperatures for January case(a), February(b) and May(c)</i>	27
6.5	<i>Diurnal variation of Wind Speed</i>	28
6.6	<i>Evolution of Wind direction</i>	29
6.7	<i>Vertical profiles of 3 days: 24Jan04(a), 25jan04(b) and a typical 19may03(c) . Each 6 hours: 00 LTC(1), 06 LTC(2), 12 LTC(3) and 18 LTC(4)</i>	32
6.8	<i>Simulated mixing-layer heights for two cases: Jan04(a) and May03(b)</i>	33
6.9	<i>Vertical profile of temperature and wind speed vectors for domain 2</i>	34
6.10	<i>Vertical profile of temperature and wind speed vectors for domain 3</i>	35
6.11	<i>Surface temperature and wind vectors for two days and 4 simulated hours for top to bottom: 00,06,12 and 18 LTC respectively</i>	37

List of Tables

4.1	<i>Terrain configuration</i>	18
4.3	<i>Physical Options chosen in the MMS modelling-system, applying to all numerical simulations in this study</i>	19
4.2	<i>Experiment desing</i>	19

Abstract

Strong wind events over the Valley of San Luis Potosi, Mexico are investigated in this research work. These recurrent meteorological phenomena characterize differently the regional climate in the winter months of January and February every year. This work is a first approximation to evaluate the atmospheric circulation over the region during the days such events last. The State of San Luis Potosi exhibits complex orographic changes, an enormous vegetation variability and diverse climate manifestations. All this special characteristics represent a challenge to be modeled considering the lack of research work done on this area. For this aim, the mesoscale numerical model MM5 was applied to simulate the mentioned strong wind events over the surface and a typical atmospheric circulation in three summer days. Reported structures associated with intense wind forcing on the surface were found on the night of January 25th such as: Low Level Jet(LLJ) patterns, Katabatic winds and gravity waves patterns. The comparison of model results with puntual observations at two meteorological stations indicate a good agreement for temperature, wind speed and direction. Additionally, the evolution of observed satellite patterns of clouds agree satisfactorily with the modeled vertically integrated column of water.

Introduction

The study of the regional climate plays an important role in the general study of the weather and climate, not only because of its importance in weather forecasting. Regional climate studies are destined to become an important tool in understanding global climate scenarios. Mainly because the possible consequences of a global climatic change supposes changes in the local patterns of rainfalls, mean temperature, start and end of an agricultural season as well as extreme events such as floods, droughts, hurricanes and windstorms. There are regions susceptible to feeling slight changes in global patterns depending on their special characteristics, geographic position, orography, vegetation cover and land use. Thus, climate change scenarios can affect determination of climate change impacts over regional crop yields while applying high and low resolution climate change scenarios to any place. It is therefore of interest to predict the potential shifts of extreme conditions in an altered regional climate^[9].

Model predictions from global climate models with such high resolutions are not likely to become widely available in the near future. Mesoscale structures that are missed by the observation network are actually, a result of land surface forcing by topography, soil moisture, surface vegetation and soil characteristics^[3].

The region of San Luis Potosi, Mexico(SLP) displays many special features: it is a zone of great orographic changes, enormous vegetation resistance and ever varying climates. Most of the area is characterized by an arid and semi-arid climate; these two sub regions characteristically have a tropical and sub-tropical vegetation, a high average temperature and moist climate. Thus, the San Luis Potosi region is largely exposed to cold fronts from the north and warm fronts from the east. It is also largely to solar radiation, and in addition orography plays an important role due to the irradiation slope, this factor is a determinant in the mesoescale process. Also, the increase of human population plays an important factor in the changes regarding land use throughout the SLP valley and the region has a large concentrated industrial development.

In order to adequately model atmospheric dynamics and thermodynamics, the fundamental physical and mathematical laws governing atmospheric circulations need to be implemented; but in a way which is physically consistent, mathematically rigorous, and computationally efficient. Simplifications regarding the scale used for the modelling, need to be carried out; these are basically conservation equations which describe the characteristics of mass, motion heat, moisture and behaviour of the pollutant species in the

atmosphere. In addition, there is a need to address any atmospheric models as well as numerous physical factors linked to the dynamical and thermal characteristics of the atmosphere. Complex interactions and feedback occur between fundamental meteorological processes; within the atmosphere itself. A multitude of complicated phenomena, ranging from turbulence and electromagnetic radiation to clouds and precipitation, require attention in models at all scales^[1]. Thus, many factors, which need to be incorporated in an atmospheric model, include the following: The nature of the underlying surface; atmospheric turbulence; solar, terrestrial and atmospheric radiation; cloud activity and precipitation processes.

Numerical Weather Prediction (NWP) provides a powerful tool, for researching many climate events such as in the case of regional ones. Mesoscale models are largely implemented worldwide and are useful too, regional climate^[21, 6, 26], boundary layer analyses^[20], severe storms^[24, 9], air quality^[14, 22] and sensitivity analyses and development of modelling^[3, 21, 27, 11] are done in order to improve the models and give them new applications.

There are many NWP models that work well depending on the scale and the specific problems that are to be studied, and cover different spatial and time scales: for example: Coupled Ocean/Atmosphere Mesoscale Prediction System (COAMPS), Advanced Regional Prediction System (ARPS), Regional Atmospheric Modelling System (RAMS), ETA model, Canadian Regional Climate Model (CRMC) and the latest and widely developed Weather Research and Forecast (WRF).

The model used in this work is the PSU/NCAR MM5 mesoscale model version 3.6 (Grell *et al*, 1994)^[10]. MM5 model does a good job in wavelengths going from 1 to 10,000 Km. In order to evaluate and compare model results with measurement data, 2 events with different local situations were chosen. There are no existing records of mesoscale applications of atmospheric models over the region of San Luis Potosi. A region with characteristics such as the aforementioned holds an enormous potential for the study of climate phenomena. This model was chosen because of its versatility to adapt to all regions of the world, its capacity to define domains with variable grid sizes and a good input resolution. Getting the input data for contour conditions may be free, but it is also a powerful tool for climate and weather analysis.

In this work, we were interested in developing and testing methods for circulating patterns of region, heat-fluxes, estimated height of planetary boundary layer (PBL), forecasting and finding the main reasons for the extreme surface wind speed presence during the winter season. In addition, sensitivity analyses of soil moisture and many parameters need to be done, otherwise the application of the MM5 becomes a simple interpolate of input data. We focused on the model outputs of wind speed and direction of two extreme wind events and compared it with a typical summertime day. These kinds of events are common in the region in wintertime.

Extreme weather events have significant impacts on the natural environment and on many socio-economic sectors. Extreme winds, for example, are of great concern because they may lead to considerable damage over forests and man-made infrastructure, as well as to the disruption of numerous socio-economic activities. Most extreme cases are defined as 'unusual events and little is known about their genesis, intensities, duration, return periods and frequency distribution^[9]. These types of events are commonly registered in the valley of San Luis Potosi during the winter months of January and February. The gusts of wind damage houses, trees, signs, etc. We have therefore chosen a couple of these January 2004 events in order to study their causes

It is obvious that obtaining realistic diurnal cycles of wind speed is important not only for NWP and cli-

Introduction

mate research, but also for studying air quality, wind energy, visibility (haze, fog, low clouds) and other environment related problems ^[27]. Diurnal wind changes to atmospheric tidal variations on the surface and differential solar heating are associated with topography, land-water contrast and cloudiness.

The correct compiling and installing of the model opens up an important line of research in the region. Observations must complement the analysis in order to obtain a correct interpretation of the results. This and the sensitivity analysis are of key importance in keeping the MM5 from becoming just a data input interpolator.

This work intends to begin a series of regional climate experiments, applying an academic approach to main regional problems such as: agriculture, prevention of disasters, air quality and weather forecasting. Hence, the contribution of this work can be summarized as follows: 1) evaluate the main aspects of atmospheric circulation over the San Luis Potosi valley, 2) Calibrate MM5 model (local characteristics) and compare it with observational data. 3) Study the recurrent wind events on winter months in special cases.

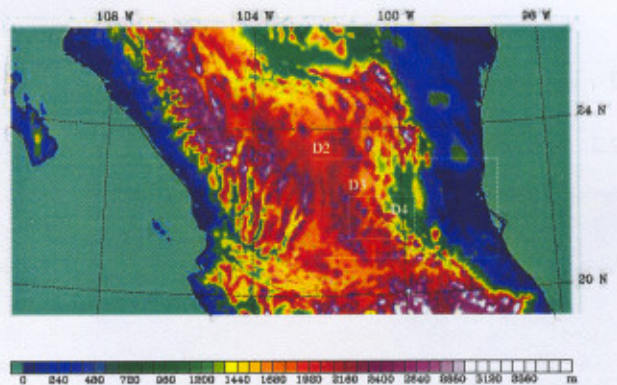
Study Zone

2.1 North of Mexico

Figure 2.1 shows the four principal domains studied here: North of Mexico (Mother domain), San Luis Potosi State (SLP)(D2), SLP Valley (D3) and SLP City (D4). Two prominent mountain chains can be distinguished in northern Mexico; the Sierra Madre Occidental on the west side and the Sierra Madre Oriental on the east. The Sierra Madre Occidental on the west is an extension of the California Sierra Nevada (with a break in south-eastern California and the extreme northern Mexico), and the Sierra Madre Oriental on the east is a southward extension of the Rocky Mountains of New Mexico and Texas. Between these two

ranges lies the Mexican altiplano (high plain). The Sierra Madre Occidental extends 1,250 kilometres south to the Rio Santiago, where it merges with the Cordillera Neo-volcanic range that runs east to west across central Mexico. The Sierra Madre Occidental lies approximately 300 kilometres inland from the western coast of Mexico at its northern end but comes up to within fifty kilometres of the coast near the Cordillera Neo-volcanic range. The northwest coastal plain is the name given to the lowland area located between the Sierra Madre Occidental and the Gulf of California. The Sierra Madre Occidental has an average elevation of 2,250 meters, with peaks reaching 3,000 meters. The Sierra Madre Oriental starts at the Big Bend region of the Texas-Mexico border and continues 1,350 kilometres as far as Cofre de Perote, one of the major peaks of the Cordillera Neo-volcanic range. As in the case of the Sierra Madre Occidental, the Sierra Madre Oriental comes progressively nearer to the coastline as it approaches its southern terminus, reaching to within seventy-five kilometres of the Gulf of Mexico. The northeast coastal plain extends from the eastern slope of the Sierra Madre Oriental to the Gulf of Mexico. The average elevation of the Sierra Madre Oriental is 2,200 meters, with some peaks at 3,000 meters. The northern altiplano averages 1 100 meters in elevation and continues south from the Northern Rio Bravo

Fig 2.1: North of Mexico Topography



through the states of Zacatecas and San Luis Potosi, where it reaches a high of about 1800-2000 meters.

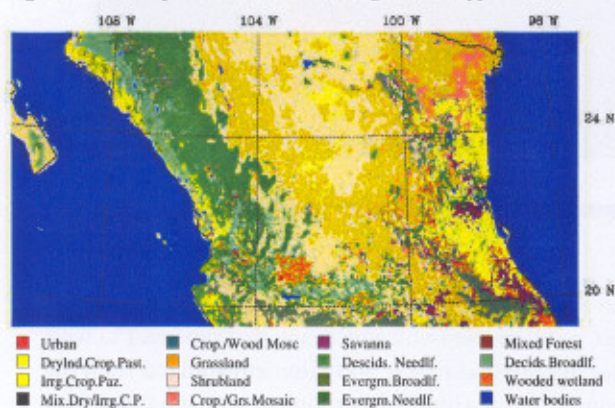
2.1.1 climate

The country is effectively divided into temperate and tropical by the tropic of Cancer. During the winter months, the land north of the twenty-fourth parallel experiences cooler temperatures. South of the twenty-fourth parallel, temperatures are fairly constant year round and vary solely as a function of the elevation. Between 1,000 and 2,000 meters, one encounters yearly average temperatures between 16 °C and 20 °C. Towns and cities at this elevation south of the twenty-fourth parallel have relatively constant, fair temperatures throughout the year, whereas more northerly locations experience considerable seasonal variations. Mexico has pronounced wet and dry seasons. Most of the country experiences a rainy season from June to mid-October and significantly less rain during the remainder of the year. Rainfall varies widely both according to location and season. Arid or semiarid conditions are encountered in the Baja Peninsula, the northwestern state of Sonora, the northern altiplano, and significant portions of the southern altiplano. Rainfall in these regions averages between 300 and 600 millimetres per year.

The geographic situation and diverse topography of Mexico lead to variable climatic regimes. The Chihuahuan Desert includes an extensive region in the north of Mexico and shows very clear changes in vegetation as we move from the lower lying regions to increasingly higher elevations. These transitions are dictated partly by changes in soil factors and partly by changes in temperature and rainfall.

2.1.2 vegetation

Fig 2.2: North of Mexico land-use Vegetation Type



The complex topography of the country, with the latitudinal and longitudinal changes creates an enormous number of environmental variants. The altitude changes produce other climatic variations of different dimensions, such as the intensity of solar radiation, atmospheric humidity, diurnal oscillation of temperature and amount of oxygen available. The most important causes of the mega diversity in Mexico are its topography, its variety of climates and its complex geological, biological and cultural history. All these important factors have contributed to form a mosaic of environmental conditions that enabled the evolution of a large variety

of habitats and life forms. The 175,000 square-mile Chihuahuan Desert extends from southeastern Arizona across southern New Mexico and west Texas. It extends south to San Luis Potosi in Mexico, bordered by the Sierra Madre Occidental on the west and the Sierra Madre Oriental to the east. This is the most important region in our study, since it is very exposed to cold fronts from the north and it is largely influenced regarding temperature and rainfall from the east and winds from the north.

Figure 2.2 shows the main vegetation types found in the region. Grasslands and shrub lands are indeed clearly dominant in the Chihuahuan desert region. This important domain includes large extensions towards the Pacific Ocean and the Gulf of Mexico. The domain applied in this research work considers

the contributions, changes and influences of the Sea Surface Temperature (SST) on the climate in the inland regions.

2.2 The State of San Luis Potosí

San Luis Potosí state is located between 24° 29' and 21° 10' north latitude; 98° 20' and 102° 18' west longitude. Have a 63,241 square-kilometer and its represent 3.1 % of Mexico surface. The northern side of the state connects with Zacatecas, Nuevo Leon and Tamaulipas; to the east with Tamaulipas and Veracruz; to the south with Hidalgo, Queretaro and Guanajuato; and to the west with Zacatecas.

The region of San Luis Potosí (SLP) displays many special features: it is a zone of great orographic changes, enormous vegetation resistance and ever varying climates. Most of the area is characterized by an arid and semi-arid climate; it is comprised by a very extensive desert region called the Chihuahuan desert, a very large portion of land, which runs from the Northern half of Mexico to the Arizona region in the United States. Moreover, the underlying surface conditions are fairly heterogeneous in this area in addition to the usual types of land use such as barren, sparsely vegetated surface, shrub lands typically found in deserts. Also the region has a large high altitude plain (1700 m) located between the two most important mountain ranges of Mexico: Sierra Madre Oriental and Sierra Madre Occidental (eastern and western Sierra Madre).

Figure 2.3 shows principal, mountain peaks on the region, the table describes names and principal elevations and its specific locations. it is possible to be seen high elevation of some peaks near than 3200 and compare with the central region or altiplano that have mean 1800 meters of altitude. In the figure are marked 3 principal regions of state: altiplano, rioverde valley and huasteca.

ID	Name	N	W	Height(m)
1	Cerro Grande	23.66	100.88	3,180
2	Sierra de Catorce	23.66	100.85	3,110
3	Sierra Coronado	23.11	100.93	2,810
4	Sierra Los Picachos del Tunalillo	23.31	101.11	2,770
5	Sierra San Miguelito	22.16	101.13	2,630
6	Cerro El Fraile	23.68	100.73	2,620
7	Picacho Las Hendiduras	22.83	101.35	2,590
8	Sierra Los Librillos	22.81	100.60	2,570
9	Sierra El Jacalon	22.58	101.25	2,500
10	Sierra Camaron	21.75	100.19	2,380
11	Picacho El Bejaco	22.51	99.61	1,960
12	Sierra El Tablon	22.31	100.35	1,840

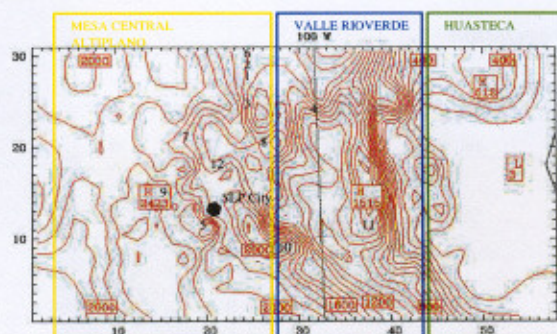


Fig 2.3: San Luis Potosí State Topography and principal Elevations(table) and its localization(figure)

2.2.1 climate

The main problem which arises while describing the climate of the region is that there are not sufficient meteorological stations and some data is disperse and incomplete. Some important factors to consider regarding this state is that the tropic of cancer passes over the central-north part of the state, the altitude variation is large and complex. The prevailing trade winds in most of the territory are a consequence of

the latitude, combined with the proximity of the sea. There is a high mountain region located toward the NE of the state of San Luis Potosí which is responsible for the way in which and cold fronts propagate southwards. Its influence produces a decrease in temperature and cloudiness.

Precipitation: 70 to 90% of the annual precipitation is concentrated between the months of May and October. The smallest quantity of precipitation is usually registered in the northern zone of the state. It has a value less than 300 mm per year. In the region of Real de Catorce, the rainfall is less than 100 mm. In the planes of the Altiplano, which represents more or less 50% of whole state, the precipitation is of 500 to 1000 mm per year. In the coastal plain, the part nearest to the Gulf of Mexico, the annual precipitation varies between 1000 and 1500 mm. The precipitation in the Rioverde Valley region, to the west of the Sierra Madre Oriental, is of the order of 1500 mm. There is a small region in the huasteca region where it reaches up to nearly 2500 mm per year. Rain is generally torrential and of a very short duration^[16].

Temperature: In the warmest region of the state in the plain coastal register annual average temperatures of 25 °C and one maximum absolute about 46 °C. In the coolest region of the state in high mountains of the north the average temperature is below to the 8 °C. The diurnal variations oscillate of the 8 to the 18 °C and estan correlated with the dryness measures. Region is a semi-dry climate in 78% of the territory due to in general evaporation exceeds precipitation in almost all the state. Temperatures varied from 24 and 26 average in zones of less than 200 meters of altitude. In Central Meseta where the height average of the 1700 to the 2200 meters the predominant temperatures vaieres of the 16 to the 18 degrees.^[16].

2.2.2 vegetation

Fig 2.4: State of SLP land-use Vegetation Type

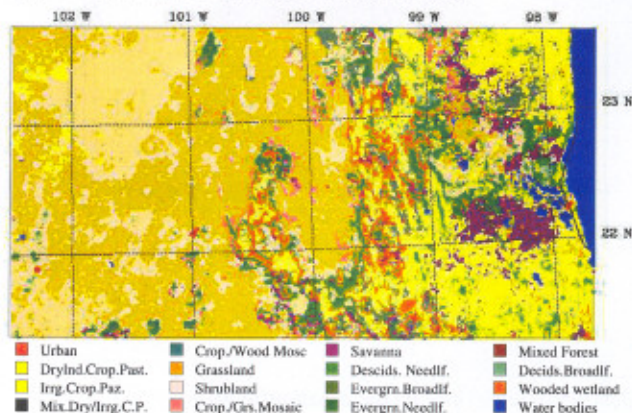


Figure 2.4 shows main the land use and vegetation for the region, as previously mentioned, the state of SLP is located, to a large extent, within the region of the Chihuahuan desert. For this reason, the type of vegetation in most of the state is scrubland covering 61.31% of the total state extension. The characteristic species are: *Opuntia streptacantha*, *Prosopis sp.*, *Larrea tridentata*, *Agave lechuguilla*, *Yucca filifera*; Croplands are second in importance and occupy 12.84% of the state extension being the principal species: *Zea mays*, *Saccharum officinarum*, *Phaseolus vulgaris*, *Capsicum spp.*, *Citrus sinensis*; Grassland is the next

most important vegetation type with a 9.84% of coverage. The typical are: *Cynodon plectostachyum*, *Panicum maximum*, *Bouteloua gracilis*, *Aristida sp.*, *Digitaria decumbens*; Tropical Forest (5.68%) is also an important component with the species: *Brosimum alicastrum*, *Bursera simaruba*, *Lysiloma divaricatum*, *Dendropanax arboreus*; Forest (6.04%) includes the species *Quercus conspersa*, *Quercus polymorpha*, *Pinus cembroides*, *Pinus pseudostrobus*, *Quercus crassifolia*; Urban Land represents 1.29% of the state region^[13].

2.3 The Valley of SLP

In figure 2.1, domain 3 (D3) corresponds to the San Luis Potosi Valley and is located in the altiplano with an approximate altitude of 1800 meters. It represents a land extension of approximately 6500 square-kilometres. The region is bordered by two important high mountain systems: to the southwest by the Sierra de San Miguelito which is a narrow plain between volcanic mountain ranges and a northeast-South eastern orientation with a maximum height of nearly 2650 meters and to the east by Sierra de Alvarez. The lack of high mountains in the northern side of the valley allows cold fronts to reach without difficulty the region. Rzedowksi (1969) ^[16] stated that the altitude of this region has an effect on the rain distribution. Additionally, the fact that the wind flows dominantly perpendicular to the mountains favours in general precipitation.

The State Capital of San Luis Potosi is 424 km north from Mexico City. It is located in the central portion of the Mexican Republic, at 22.153 ° north latitude and 100.98° west longitude, rising to an altitude of 1877 meters. The population of SLP city is aprox. 850,000. This represents 36% of the state of SLP. The city is over 400 years old; with mining -mostly silver and zinc playing an important role in the development of the city. In our days the mining industry represents one of most important economical sources and development in the region. But there are other industries located to the east of the city and these represent a significant source of pollution.

The city itself also has many special regimes of wind, floods and many other seasonal manifestations of weather conditions. In winter, it experiences more that 20 cold front coming from the north. In summer, warm front reaches the region from the east.

Synoptic Situations

Figure 3.1 describes the position of a front separating a cold air zone in the north and a region of warmer air in the southern part of Mexico. The front moved slightly southwards in the considered days. This cold front is associated with a rain zone which extends along the front and flows to the northeast. This synoptic situation generated strong pressure gradients along the front with low pressure zones in the north and high pressure in the southern part of Mexico. From this meteorological front system arose a very strong wind circulation which generated through the interaction with the orography wind velocities of about 50-60 Km/h. The maxima wind intensity was reached between January 24th at 12:00 local time and January 25th at 6:00. This can be seen in figure 3.1(d), where the front system has evolved to a situation where several high and low pressure regions can be distinguished. The low pressure area, located over the southern part of the United States and the high pressure region over the Gulf of Mexico favours decidedly the intensification of the severe wind event over the central part of Mexico. These synoptic situations occur recurrently in the winter months of January and February every year. The analysis on the build up of this synoptic conditions and the consequences on the circulation over a very complex orography could help to prevent damages in crop lands and man-made infrastructure.

The region of most interest in this study is located, in this particular case, precisely at the boundary of the cold front and consequently in the zone of strong pressure gradients and major wind intensities. The principal aim of this investigation is to reproduce through numerical modelling, the conditions of strong wind forcing events and the consequences of such synoptic systems over the State of San Luis Potosi, Mexico and particularly over the Valley of San Luis Potosi. The general distribution of physical parameters associated with this synoptic systems were applied to initiate the simulation and to interpretate the results.

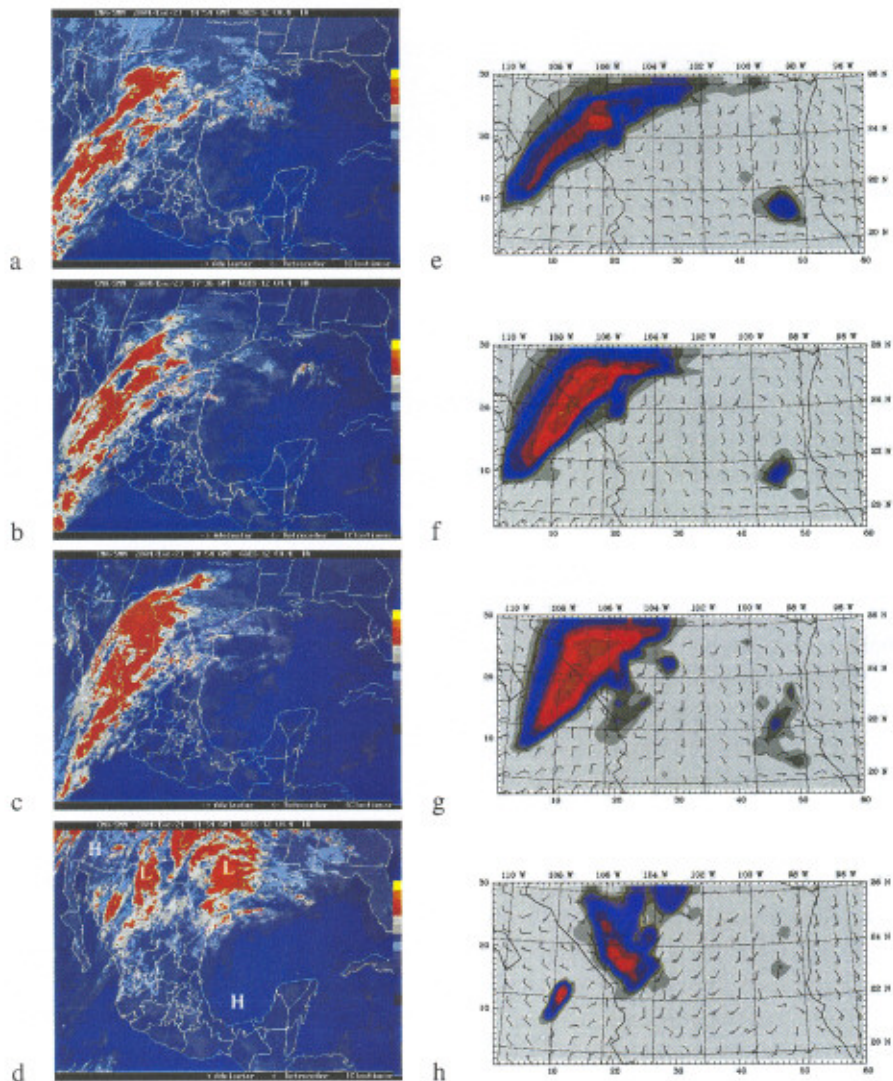


Fig 3.1: Evolution of the front system over north Mexico on January 23th and 24th of 2004 from satellite infrared data (left side)(source: Servicio Meteorologico Nacional CNA) . Results of the modeled column of water (righth side)

4

Methodology

In order to present a good climate description on a specific region such as the San Luis Potosi Valley, it is necessary to be familiar with all processes involved, such as physical and chemical. It is also of fundamental importance to have a knowledge concerning dynamic fluxes, forcing systems and boundary conditions. We need to introduce conservation laws equations; the hydrodynamic equations of Navier-Stokes, the continuity equation for mass conservation, the diffusion-advection equation for temperature and other governing equations for substances like water vapour and pollutants.

To calculate the dynamics in an atmospheric system, it is necessary to solve mathematically the complex non-linear equation of motion. It is possible to carry out simplification and parameterizations to get analytically information on the different kind of waves contained in the general equations. In theory, then, we can use these equations to create a mathematical model of the atmosphere, with initial and boundary conditions based on data from the past and current state of the atmosphere, and solve the equations to predict a future state. In the praxis the system of equations can not solved analytically, since the topography is complex and the equations of motion are non-linear in nature. A way to solve the equations in the most general and possible form is the application of numerical methods. Therefore, laws are expressed in a mathematical form and solved numerically, but based on initial observations.

Atmosphere motion can be described mathematically by using a Numerical Weather Prediction (NWP) computer model. NWP Models work by mapping a mathematical description of the atmosphere onto a three-dimensional computational grid. The state of the atmosphere is then calculated (forecasted) at each point on the grid for given steps of time into the future. These time steps are typically in the order of several minutes, while the total time span of the computer forecast may range from one to five days, or more, into the future.

Some physical phenomena like turbulence and clouds formations are too difficult to describe mathematically. For this reason the involved variables are decomposed in mean and perturbation variables. The substitution of these variables in the primitive equations leads to closure problems which are resolved by introducing some parameterizations as functions of the mean variables. To model all these parameterizations is necessary to carry out a lot of measurements to adjust and calibrate the constants appearing in the new equations, for example to estimate the coefficient of turbulent diffusion of moment. In other

words, in the parameterisation process, some constants are introduced in the equations; these constants are estimated and calibrated with data originated through observational experiments.

This work intends to start a series of analysis of regional climate events and combine observations with numerical simulations over the SLP Valley. The region previously described, presents special characteristics such as orographic features and different vegetation types and therefore poses the opportunity for a good research.

Mesoscale meteorological models can now provide input on horizontal grids with dimensions of 10 Km or less, making them useful in complex terrain, urban, costal, and other spatially inhomogeneous geographical regions. Models run sufficiently so they can be used for real-time predictions. Simulations of temperature, wind speed, direction, radiation, pressure, potential temperature and others could be compared with observations made at surface meteorological stations and Radiosondes.

4.1 MM5 Model description

The PSU/NCAR mesoscale model is a limited-area, non-hydrostatic, terrain-following sigma-coordinate model designed to simulate or predict atmospheric circulation at a mesoscale and regional-scale. It has been developed at Penn State and NCAR as a community mesoscale model and is continuously being improved on by contributions from users at several universities around the world. The Fifth-Generation NCAR / Penn State Mesoscale Model (MM5) is the latest in a series which developed from a mesoscale model used by Anthes at Penn State in the early 70's and was later documented by Anthes and Warner (1978). Since then, it has undergone many changes designed to broaden its usage. These changes include (i) a multiple-nest capability, (ii) non-hydrostatic dynamics, which allows the model to be used at a few-kilometre scale, (iii) multitasking capability on shared- and distributed-memory machines, (iv) a four-dimensional data-assimilation capability, and (v) other physical options.

MM5 is used worldwide for many and very diverse applications: Regional Climate^[15], Analysis of past severe events like convective^[24, 26] or wind storms^[2, 6], Planetary boundary layer studies^[21, 27, 20], Air Quality^[22, 23, 14] and many others.

4.1.1 Governing Equations

For MM5 mesoscale model governing equations are: perfect gas law, conservation of mass, conservation momentum, conservation of heat, water and other gaseous materials or aerosols.

The vertical σ -coordinate is the defined entirely from the reference pressure, this transformation is important in order to describe pressure levels function of terrain conformation and is defined by follows:

$$\sigma = \frac{p - p_t}{p_s - p_t} = \frac{p - p_t}{p^*} \quad (4.1)$$

When p_s and p_t are the surface and top pressures respectively of the model, where p_t is a constant.

Conservation of mass are defined by:

$$\frac{\partial \rho}{\partial t} + \frac{\partial}{\partial x_j} (\rho u_j) = 0 \quad (4.2)$$

and conversion of a scalar:

$$\frac{\partial \Psi}{\partial t} + u_j \frac{\partial \Psi}{\partial x_j} = S_\Psi \quad (4.3)$$

Where Ψ is a generic scalar that represents temperature, water variables, gaseous or aerosols substances and the symbol S_Ψ represents the sources and sinks of each variable.

MM5 includes a non-hydrostatic equations, this is important because non-hydrostatic effects are essential in atmospheric phenomena, many forces and exchange flows are developed under this scheme. The deviation from this equilibrium describes the non-hydrostatic part in the vertical equation of motion. The introduction of this approach allows simulating processes with a space scale of a few kilometres.

For non-hydrostatic model the equations are redefine in two components: reference state and the perturbations from it, as follows:

$$\begin{aligned} p(x, y, z, t) &= p_0(z) + p'(x, y, z, t) \\ T(x, y, z, t) &= T_0(z) + T'(x, y, z, t) \\ \rho(x, y, z, t) &= \rho_0(z) + \rho'(x, y, z, t) \end{aligned}$$

With the previous transformations and applying equation (4.1), the reference state are independent of time. Total pressure at a grid point is therefore given by:

$$p = p^* \sigma + p_t + p' \quad (4.4)$$

Where $p^*(x, y) = P_s(x, y) - p_t$. The three-dimensional pressure perturbation, p' is a predicted quantity. The model equations (dudhia, 1993)^[7] are given by the following:
Pronostic equation for pressure perturbation p' ;

$$\frac{\partial p'}{\partial t} - \rho_0 g w + \gamma p \nabla \cdot \vec{v} = \vec{v} \cdot \nabla p' + \frac{\gamma p}{T} \left(\frac{\dot{Q}}{c_p} + \frac{T_0}{\theta_0} D_\theta \right) \quad (4.5)$$

Horizontal momentum;

$$\frac{\partial u}{\partial t} + \frac{1}{\rho} \left(\frac{\partial p'}{\partial x} - \frac{\sigma}{p^*} \frac{\partial p^*}{\partial x} \frac{\partial p'}{\partial \sigma} \right) = -\vec{v} \cdot \nabla u + f v + D_u \quad (4.6)$$

$$\frac{\partial v}{\partial t} + \frac{1}{\rho} \left(\frac{\partial p'}{\partial y} - \frac{\sigma}{p^*} \frac{\partial p^*}{\partial y} \frac{\partial p'}{\partial \sigma} \right) = -\vec{v} \cdot \nabla v + f u + D_v \quad (4.7)$$

Vertical Momentum;

$$\frac{\partial w}{\partial t} - \frac{\rho_0}{\rho} \frac{g}{p^*} \frac{\partial p'}{\partial \sigma} + \frac{g}{\gamma p} p' = -\vec{v} \cdot \nabla w + g \frac{p_0}{p} \frac{T'}{T_0} - \frac{g R_d}{c_p} \frac{p'}{p} + D_w \quad (4.8)$$

Temperature;

$$\frac{\partial T}{\partial t} = -\vec{v} \cdot \nabla T + \frac{1}{\rho c_p} \left(\frac{\partial p'}{\partial t} + \vec{v} \cdot \nabla p' - \rho_0 g w \right) + \frac{\dot{Q}}{c_p} + \frac{T_0}{\theta_0} D_\theta \quad (4.9)$$

4.2 Model Configuration

4.2.1 Terrain Configuration

Version 3, release 3.6 of non-hydrostatic Penn State University National Center of Atmospheric Research Mesoscale Model MM5^[7, 10], is being used for this study. Basic standard configurations were running with 4 domains. Centered at 21 degree N latitude and 101 degree W longitude, covering northern center of Mexico. A 27-Km coarse grid domain covers the north of Mexico with a domain size area of 1620 Km × 810 Km. Three

MM5 Domains	D1	D2	D3	D4
Horizontal Resolution (Km)	27	9	3	1
East-West grid points (#)	60	58	40	31
North-South grid points (#)	30	31	31	31
Vertical σ Levels	47	47	47	47
Time Step (seconds)	81	27	9	3

Table 4.1: Terrain configuration

inner domains –two way nested– are placed inside the coarse domain, use resolution of 9, 3 and 1 Km. The second 9 Km grid domain covers all of the San Luis Potosi State near the ocean boundary, resulting in a domain size area of 522 Km × 279 Km. The third one covers the San Luis Potosi Valley (our area of interest), in which the smallest one is centered in the city of SLP where there are two weather observation stations, resulting in domain areas of 120 Km × 93 Km and 31 Km × 31 Km in size, respectively. Figure 4.1 shows the three inner domains over the valley of SLP and figure's borders representing the coarse domain. 30 seconds resolution database of the U.S. Geological Survey (USGS) are used for each domain to establish for initial conditions of topography and land use. For summer and winter conditions 1 Km 25 Category land-use for USGS are used to calculate the following: Albedo, Moisture, Emissivity, Roughness Length and Thermal Inertia. Lambert conformal is used for making a Map projection. Table 4.1 shows all terrain configurations.

4.2.2 Boundary Conditions and Vertical Configuration

The REGRID model input datasets are obtained from NCEP Global Analysis on 1x1 degree resolution that cover the entire globe every six hours. This data is in GRIB format and has all the meteorological variables that the model needs, Time varying sea-surface temperatures were taken for this set also. For Upper Air Observation ds053.4 NCEP dataset are used and ds064.0 dataset for the surface observations, with this dataset inputs for LITTLE_R are obtained. For INTERPF main program 47 σ levels in a non-linear configuration, in fact have more resolution (around 35 mt) near the surface up to 1000 meters, soon the intervals are but great. This configuration allows us to have much more data in the first layers of the atmosphere, where the events, which are of interest for us for, are occurring; these include: fronts, extreme winds, heat fluxes and temperature gradients. Because a fine vertical resolution like the one used here enhancement helps to better simulate the boundary layer that modulates the wind speed along the surface and represents the atmospheric circulation better with a very complex structure^[9].

4.2.3 MM5 Configuration and physical options

Numerical experiments were running on 2 processor Compaq Tru64. Distributed Memory Extension configuration was used to compile and run the main program MM5 with an MPP option. Default settings of MM5 were used to create most of the simulations. Table 4.3 shows the main physical options which were applied.

Domain	1	2	3	4
Basic Model Configurations				
Cumulus Scheme(ICUPA)	Grell	Grell	Grell	Grell
Moisture Scheme(IMPHYS)	Warm Rain	Warm Rain	none	none
Radiation Scheme(IFRAD)	Cloud-Rad	Cloud-Rad	Cloud-Rad	Cloud-Rad
Surface Scheme(ISOIL)	Five-Layer	Five-Layer	Five-Layer	Five-Layer
PBL Schemes(IBLTYP)	Blackadar	Blackadar	Blackadar	Blackadar

Table 4.3: *Physical Options chosen in the MMS modelling-system, applying to all numerical simulations in this study*

Three events were chosen for this study, two in wintertime and one in the summer. The events in winter were chosen because strong winds occur over the surface; these events are typical and periodical every year in the months of January and February. The summer event was chosen to compare other events with a typical summer-time situation. A three-day numerical experiment was simulated in each case. Table 4.2 shows the specific days. All experiments start running at 00 Universal Time (UTC), 18 Local time (LTC). In any case all the simulations ran for 72 hours, pair to use the first day like *spin-up* and in the following ones to evaluate the true evolution of the model. Complete 3-day diurnal cycles are simulated. In this way, the may experiment represents a typical summer day with high radiation fluxes and ground temperature cycles. On the other hand the study gave the January event a special attention, i.e., this investigation is focused on these events. Many sensitivity analyses were made before running definitive experiments and they are shown in the next chapter. Finally, typical MMS parameterisations were chosen.

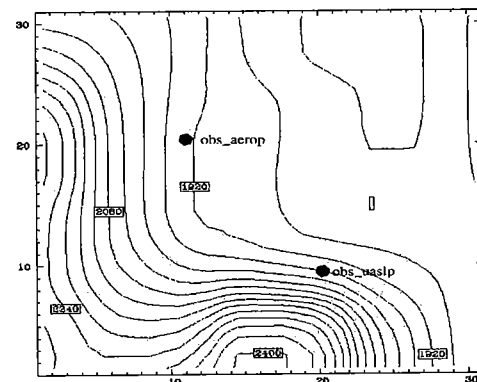
Experiment	season	Period
E. #1	Winter	23-26 Jan
E. #2	Winter	22-25 Feb
E. #3	Summer	18-21 May

Table 4.2: *Experiment desing*

4.3 Observations

It has been widely accepted that modelling of land surface processes plays an important role in mesoscale numerical models of the atmosphere. But in order to carry out a reliable study with simulations; these must necessarily adjust to the observed data. San Luis Potosi is a city with a small infrastructure regarding meteorological observation. The data are dispersed and insufficient. There are a few long-term data records, but with only a few meteorological variables. There are two reliable sources of data; from the ‘**Ponciano Arriaga**’ international airport of San Luis Potosi (airport_obs), located at 22.1° N 101.01° W. These sets of data are written in METAR code and at 1 hour time steps. The second is from a fixed meteorological station at the Instituto de Zonas Deserticas, which belongs to the University of San Luis Potosi (UASLP_obs). This data set is written on the simple ASCII code and at 10-minute time steps.

Figure 4.1: *Observational Stations*



The near-surface observations, obtained at these two stations, were used to evaluate the accuracy of the calculated 2-meter temperature, mixing ratio and 10-meter winds. In both cases, the data set contained the following meteorological fields: temperature, dew point, relative humidity, wind speed and wind direction. Pressure and radiation parameter were also included in the data sets. The model permits us to obtain time series of any meteorological variable at any mesh point, in this way we can convert all grid points of the model in virtual observational meteorological stations.

Sensitivity Analysis

The MM5 model can be applied to carry out studies around the world. In this process, the model parameterisations are performed automatically and to some extent have a general nature. This supposes a problem when specific studies over a determined region are necessary. Land surface models and their parameterisations are important for making realistic simulations on the diurnal and vertical structure of Planetary Boundary Layer (PBL) processes.

The inclusion of the new LSM in MM5V.3 is with the purpose of improving and mitigating the slab soil model in MM5V.2: 1) constant soil moisture field, 2) relatively coarse resolution of land use maps, and 3) no vegetation evapo-transpiration nor runoff process. There has been a great progress regarding the development of new techniques and finer mesh grid sizes. But in mesoscales, when the MM5 grid increase is over 1Km, the dominant vegetation type in each grid box represents the characteristics of the 'grid level' vegetation^[3]; the albedo and roughness length are specified according to the given dominant vegetation type.

Thus, a surface layer parameterisation should provide the surface (bulk) exchange coefficients for momentum, heat, and water vapour used to determine the flux of these quantities between the land surfaces and the atmosphere.

Soil moisture is a very important component of land surface modelling, and it would not make any sense to implement a sophisticated LSM in mesoscale models without a proper initialisation procedure of soil moisture. However, the initialisation of soil moisture in coupled regional models is geoparded due to the fact that there are no routine soil moisture observations of high resolution soil moisture at large scales. Secondly, there because precipitation and surface radiation are not restricted (or assimilated), in the traditional four-data assimilation systems, the soil moisture fields suffer model errors in radiation and precipitation. For instance, the ECMWF operational global model had problems related to large drifts in soil moisture, which in turn, affected the precipitation forecast^[3].

MM5 has fixed values for initialisation of soil moisture, for the grassland use type, this value is 30%. Grassland mainly covers the region of San Luis Potosi although presenting dry and arid characteristics. Thus, MM5 sets at 30% soil moisture, but this value is overestimated in this region. There are no large

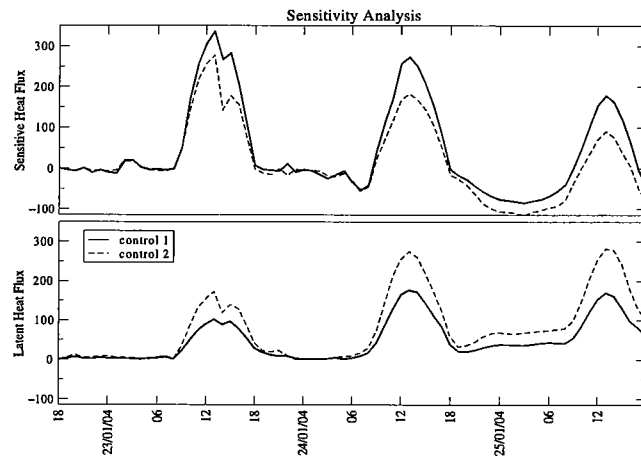


Fig. 5.1: Sensitivity analyses for two soil moisture values

networks of observed data available of this parameter. Nevertheless, some isolated data indicates that the soil moisture value in the grassland vegetation type almost never reaches levels of 15%. This value is important for considering the heat flows. This behaviour was previously described by Chen et al (2000) who stated, 'a perturbation in initial soil moisture seems to primarily affect the surface energy balance in dry and semiarid areas. Furthermore, the initial soil moisture fields, especially in arid and semiarid climate regions, also significantly influence the partitioning of surface radiation forcing into latent and sensible heat fluxes^[3]'.

The responses of the surface heat flux of the model to the initial moisture changes are shown in fig.5.1 for both soil moisture values 30% (dashed) and 15% (solid) on a grassland surface point. We can clearly see a decrease of latent heat fluxes and an increase, by conservation, in sensitive heat. In any case, the negative values of the sensitive heat remain; something we will study afterwards. Also, sensitivity analysis were made to evaluate the response of the model to different PBL parameterisations as well as changes in rough length (not shown here), but no significant differences were found in the fluxes for these changes.

Results and Discussion

6.1 Radiation Budget

The region of the San Luis Potosí Valley is exposed to strong radioactive forces whose intensity is important to know. In this process, the surface administrates the radiation received from the sun and influences the layers above it, so that the climatology and the way the surface administrates the radiation are closely related. A problem arises as we try to associate the relationship between the fluxes on the surface to a single factor (i.e. soil, vegetation cover, etc.) because the top surface conditions are fairly heterogeneous over the studied area.

Almost all simple grid point analyses have been done in a grassland environment. However, there is also great influence from the shrub land. This land-use types are generally unproductive with a sparsely vegetated surface. This of land use is found in the San Luis Potosi Valley. Additionally, due to the orographic complexity of the region, implicit differences exist in the energy budget due to the differences in slope irradiation. Slope irradiation analyses were included in the MM5 model by Grell^[10].

Figure 6.1 shows diurnal evolution of simulated radiation forces: incoming Short-wave solar radiation ($K \downarrow$), incoming Long wave ($L \downarrow$), Net Radiation (Q^*), Short-wave reflected solar radiation ($K \uparrow$), Long wave up from ground ($L \uparrow$) and observations (obs_uaslp). There is a clear difference between a winter month (a) and a summer like month (c). The January graph (a) shows differences in the K in components in comparison to May (c). These differences can be associated with cloud events in the January days and simply differences in solar elevation, i.e. the relative inclination of the sun in the different simulated days. In all cases, long wave radiation L_{in} and L_{out} appears to be nearly constant, with little diurnal variation. This can be expressed in the following equation:

$$Q^* = K \uparrow + K \downarrow + L \uparrow + L \downarrow \quad (6.1)$$

This simulation provides a good agreement between $K \downarrow$ and observational data in the May and January months near sunset. However, the calculated data presents a strange behavior which can be distinguished in small peaks found in all simulated January days. The January chart shows low intensity of short wave incoming radiation at 12 LTC of the last day. The chart for May (c) indicates that incoming solar radi-

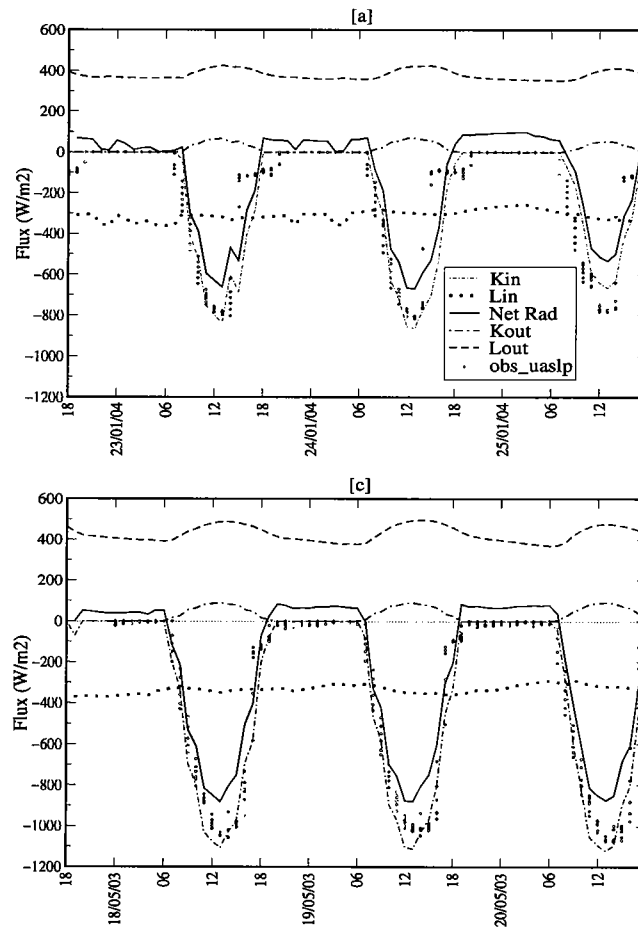


Fig. 6.1: Surface Radiation Budget Components for two cases: January case(a), and May case(c)

ation reaches values close to $1100 W/m^2$ around 12(LTC). These values are near to that solar constant, and they are indicating the enormous radioactive force over the ground during these days. However in all cases Long and short wave outgoing radiation shows the same behavior in both charts.

6.2 Turbulent Fluxes

Figure 6.2 show the simulated diurnal cycles of sensitive heat flux (SHF), latent heat flux (LHF) and friction velocity (UST) for two simulations: January (a) and May(b)cases. In all cases the maximum value occurring between 12 and 13 LT, in the May case sensitive heat flux is close to $400 W/m^2$ and it shows a normal evolution of heat fluxes in a three day simulation, latent heat flux is near $200 W/m^2$, friction velocity (UST) values are small and show a typical diurnal evolution.

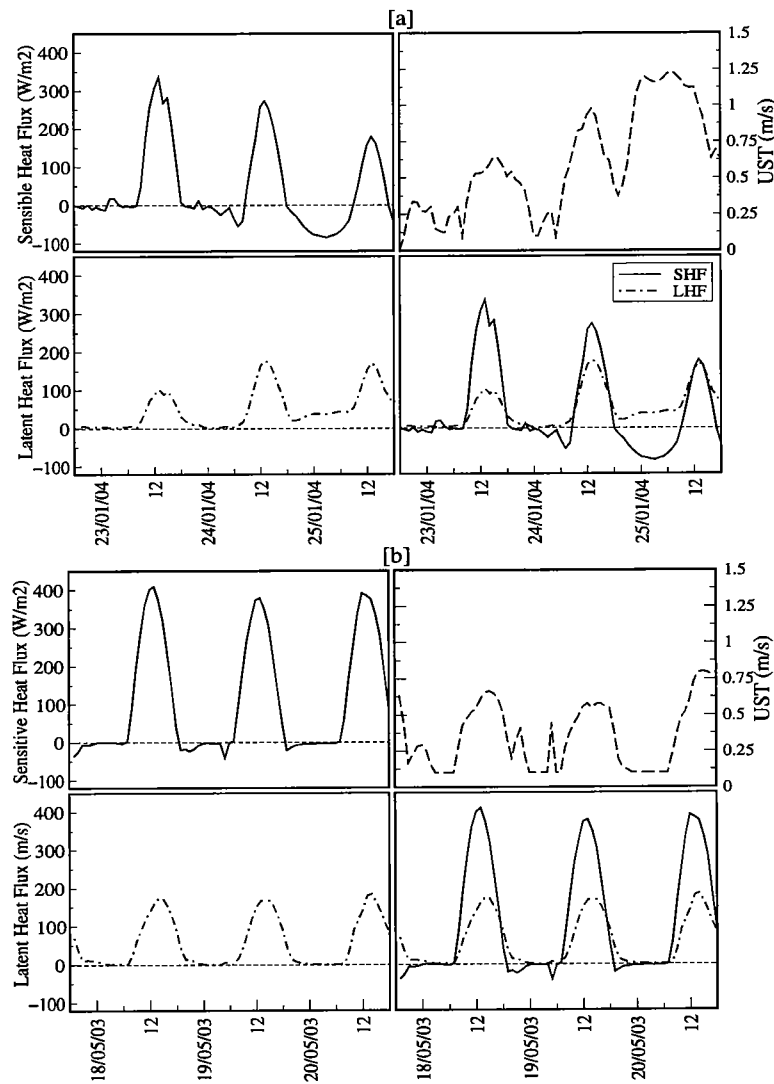


Fig. 6.2: Time evolution of Heat Fluxes and Friction Velocity

The behaviour of the time series in the January case (a) shows large differences in comparison with the May case in all simulated variables. Maximum values are around 12 and 13 LT, but for the first day this value is about 350 W/m^2 , on the second day, this value falls below 300 W/m^2 . For the last simulation day (Jan 25), the maximum value of SHF does not reach 200 W/m^2 . On the other hand, the diurnal evolution of the LHF shows a slight increase regarding the maximum value of 100 W/m^2 , on 12 LTC of January 23. It reaches values close to 200 W/m^2 at 12 LTC of January 25. Friction velocity has an increase in its value with diurnal evolution; at midnight of Jan 25 it reaches values close to 1.5 m/s . The friction velocity (U), which is related to the wind speed (M_a); the temperature difference ($\theta_g - \theta_a$) for SHF and the moisture difference [$q_{vs}(T_g) - q_{va}$] for LHF.

Another important observation is the very negative value of the SHF during the night of day 25. It is a value close to -100 W/m^2 . This kind of cooling may be caused by many factors such as wind strength. Figure 6.3 shows a comparison between the friction velocity (UST), wind speed and the difference between soil temperatures and the first simulated atmospheric layer. We can say that that the strong wind forcing on the surface helps to increase the ground rate of cooling compared to normal conditions without an associated strong wind.

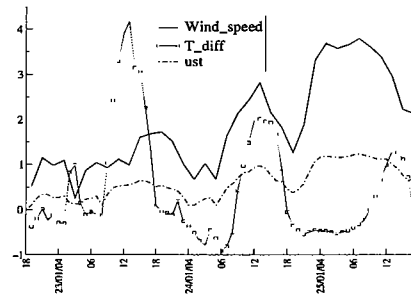


Fig. 6.3: Comparison of UST, wind speed and T difference

Unfortunately, there is not *in situ* observational data to compare with the simulated values. There may be a tendency to overestimate the values by the model, a fact that was previously reported^[3, 21]. On the other hand, the fair weather conditions associated with clear skies and strong nocturnal radioactive cooling are also associated with anticyclones, divergence and subsidence.

Surface layer parameterisation should provide the surface (bulk) exchange coefficients for momentum, heat, and water vapor used to determine the fluxes of these quantities between the land surface and the atmosphere. As we saw previously, the partitioning of surface radiation forcing into latent and sensible heat fluxes is also significantly influenced by the initial soil moisture fields, and a disturbance in initial soil moisture seems to primarily affect the surface energy balance in arid and semiarid areas^[3].

6.3 Observations

6.3.1 Temperature

Figure 6.4 shows a comparison of the diurnal variations of surface temperature between 2 sources of observation: UASLP (points), Airport (dash and plus) and MM5 simulations (solid). Two different cases are described for a January situation (a) and May situation (c). The agreement between observations and simulations is good considering international standards. Calculated and observed time series of temperature are very well correlated in the diurnal cycles. However, in general, surface temperatures obtained with the MM5-model simulations are underestimated in comparison to the observations. Discrepancies in the simulations could be caused by many factors such as PBL parameterisations, horizontal diffusion, model set-up and boundary conditions (Hauge, 2002)^[12]. The temperature near the surface depends closely on the local physical grid point properties that we are simulating such as albedo and emissivity and it can easily be advected to other areas (Zang, 2004)^[27]. Another source of errors is the deficiency on input datasets (Otte, 2001)^[14]. Reports indicate that a good weather forecast is attained in within a margin of error of within $2 \text{ }^\circ\text{C}$ of observations (Hanna, 2001)^[11].

6.3.2 Wind Speed and Direction

Figure 6.5 shows the diurnal evolution of wind speed for 2 cases: extreme case in January (a) and typical case in May(c).

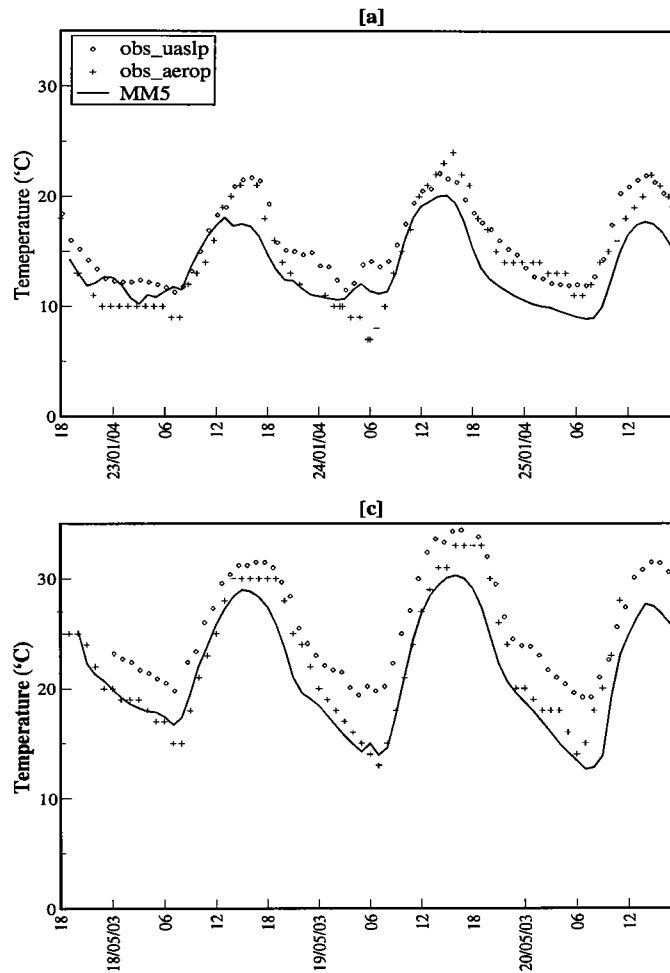


Fig. 6.4: Diurnal variation of Temperatures for January case(a), February(b) and May(c)

The January situation shows clearly an increase of the wind speed towards the end of the simulation. Simulations and observations are relatively well correlated in the first part of simulation and show large discrepancies in the last day. On May 24th the wind reached a maximum speed whose variability could not be appropriately simulated by the model. Furthermore, wind speed and diurnal cycles of heat flux are not well correlated as one would expect^[27]. There is a lot of work in this direction to do in the future. To adjust the model to the most real possible situation is necessary to carry out experiments to measure all these physical parameters.

For the May situation, the figure shows the typical diurnal cycles and light decrease of the maximum wind speed. The analysis of the results of all these numerical experiments reveals that the values of the parameters applied and the schemes introduced in the model modelling underestimate the strength of

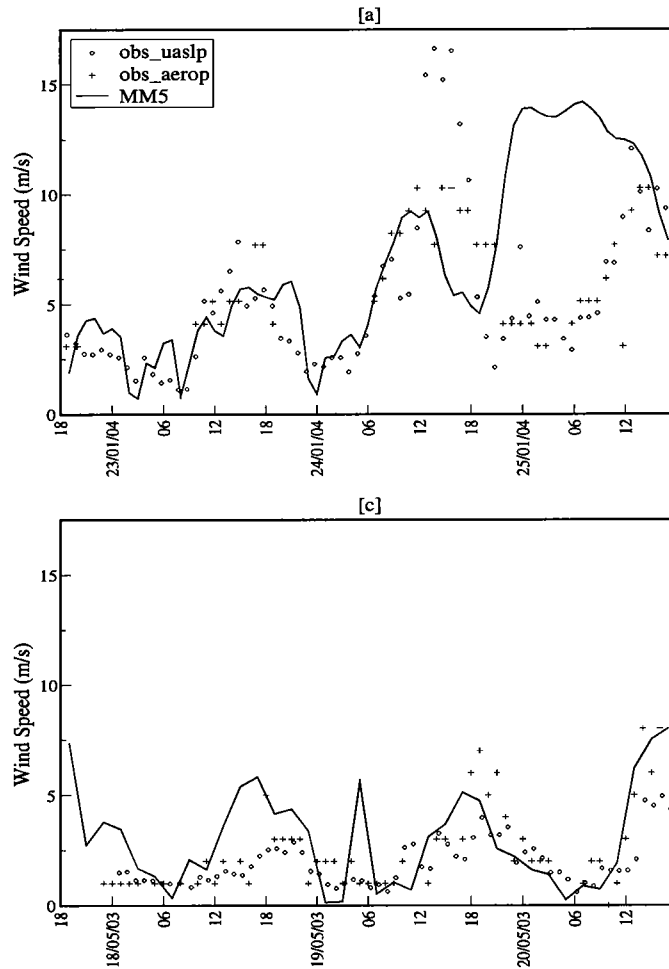


Fig. 6.5: Diurnal variation of Wind Speed

wind speed during day time, and overestimate it during nighttimes^[27]. However, the order of magnitude and accuracy of the predicted wind speeds and directions give a first trustworthy approximation of the wind system in the Valley of San Luis Potosi.

The results indicate that good simulations of the diurnal surface temperature cycles do not necessarily guarantee us that the diurnal cycles of wind speed will have the same satisfactory behaviour. Wind speed forecast were usually within 2.5 ms^{-1} in relation to observations^[11]. These results suggest that the influence of the parameters is greater on wind fields than in temperature fields. Moreover, wind observations are typically a snapshot of winds occurring at the time and may not reflect the strongest winds that have occurred since the last observations^[6]. The simulated wind speed generally represents a short term average on the hour. Observed in situ, meteorological variables such as wind speed are affected by stochastic fluctuations in wind speed and spatial variability within the grid square. There are many factors that can influence the observed wind values that can not be taken in account in the model like building, streets,

trees, etc. However, there are differences to be expected between the observations and the simulations due simply to the differences of the average volumes and average times that they represent (Hanna, 2001)^[11]. Discrepancies could be also induced by simple limitations and implicit error associated with both observations and model data (Dailey, 2002)^[6].

This kind of extreme wind events in the surface layer in the San Luis Potos  Valley, which are investigating, can be related with instabilities at the top of troposphere. This instabilities can be attributed to many factors like: convective events, turbulent transport from the top of boundary layer to surface (Brausser, 2001)^[2], slope irradiance (Hauge, 2002)^[12], gravity waves activity (Dailey, 2002)^[6], Katabatic winds, low level jet and Kelvin-Helmholtz instability^[19]. In the following sections, we analyse these effects for our case study with wind profiles and low-level jet analysis.

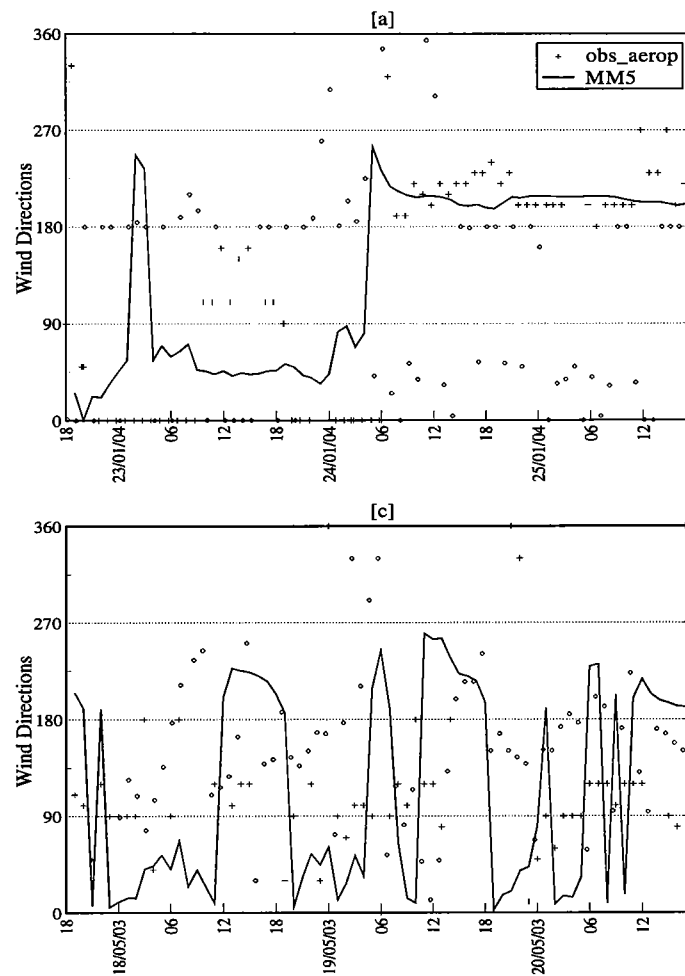


Fig. 6.6: Evolution of Wind direction

Figure 6.6 shows the diurnal evolution of wind direction for the January and May situations. In the Jan-

uary calculation there is a good agreement between model simulations and airport observations. However, in comparison with the UASLP observations there are more discrepancies. In this last case, the NE direction is the predominant one, when the wind speed is at a maximum. For the May situation (c), a defined pattern does not exist, the wind strength is weak and there is not a clear tendency of the wind direction. In general, in the presence of small wind intensities, stochastic events are dominant, making it difficult to make an accurate forecast.

Several factors may explain the difficulties in reproducing the anemometer level mean wind speeds and gust. The first is related to problems of measurement, i.e. of how and where climate instruments are located. Anemometer levels are located at different heights depending on the local geographical situation, which may well differ from that in model. The measured wind speed may also be biased because of site characteristics. The measured height may vary from the near surface to hundreds of metres, so that the measured and calculated wind speed may significantly differ.

Wind channelling may accelerate winds to produce gusts that last a few seconds to a few minutes. The second factor is attributed to the parameterisation scheme that is employed to compute surface winds in models^[9]. A good report for wind modelling would be close to a 15% of similarity to the one observed, further in such wind situations, wind directions are known to be variable and unreliable [11]^[11]. Other authors report that wind directions are usually forecasted within 30° (Zhang, 2004)^[27]. The simulations carried out in this investigation satisfy satisfactorily these standards.

6.4 Planetary Boundary Layer

The PBL is defined as a part of the atmosphere or more particularly of the troposphere that is strongly influenced directly by the presence of the earth surface, and responds to surface forcing with a timescale of an hour or less^[19]. In order to understand the generating processes of the wind events on the surface it is necessary to understand the structure, behavior, and evolution in the time of Planetary Boundary Layer. Surface forcing process like: heat fluxes, soil moisture, vegetation transpiration and cover, albedo, topography, roughness and soil characteristics roughness take special importance in the mechanics or convective turbulence.

The atmospheric boundary layer is inherently turbulent. Having an idea of the form in which the turbulent processes happen allows us to infer typical structures of winds and temperature in the vertical dimension. Boundary wind can be divided into three parts: mean wind, waves and turbulence. In the boundary layer, horizontal transport is dominated by the mean wind and vertical by the turbulence. PBL is usually shallower in the high-pressure regions due to the descending motion, pushing the PBL top down. PBL horizontal divergence also decreases the height^[19]. SBL winds can have very complex characteristics; in the lowest 2-10 m wind direction and evolution depends on the local topography, the buoyancy effects, the friction intensity and on the entrainment.

6.4.1 Vertical Profiles

Figure 6.7 shows vertical profiles of potential temperature and wind speed for 3 days: January 24(a), Jan25 (b) and May19(c). Each chart shows vertical profiles for 00(1), 06(2), 12(3) and 18 LCT (4). The figures show a special event on January and a typical heat day situation like in May 2003. This simulation has been carried out to have a control or reference simulation experiment. At 00 LT of 24 day, chart (a.1) shows a typical normal wind and temperature profile with calm wind speed on surface. In the next time

step, figure (a.2) shows an increase in the wind speed field reaching values of 5 m s^{-1} in ground level, a change in a vertical profile that reaches values of wind speed above 20 m s^{-1} , 900 m over the ground. The general shape of the vertical profile remains until 18 LT of 25 day, reaching a maximum value (near than 30 m s^{-1} at 650 mt over surface) on 06 hour of 25 day. This perturbation increases wind speed surface levels with values and time evolution described before. On the other hand, the vertical profiles for the May situation show nocturnal inversion of temperature and little wind speed, in particular chart c.3 (12 LTC) shows a well-mixed layer with a 2 Km height.

These kinds of events are called Low Level Jet (LLJ), and are largely reported in literature. These events are typically nocturnal, but also occur during daytime. They are characterized by a thin stream of fast moving air, with maximum wind speeds of 10 to 20 m, which is usually located 100 to 300 m above the ground and are not a rare phenomenon^[19]. Goyette *et al.* (2001) reports that in the Swiss Alps low level jets reach wind speeds of more than 45 m s^{-1} , located below 1000 m above the surface^[9]. There are many possible causes for LLJ: synoptic-scale baroclinicity associated with weather patterns, baroclinicity associated with sloping terrain, fronts, advective accelerations, splitting, ducting and confluence around mountain barriers, land and sea breezes, mountain and valley winds and internal oscillations^[19]. Brauseur has reported that wind gusts associated with storms over Europe are characterized by the turbulent transport from the top of boundary layer to surface^[2].

6.4.2 Stable Boundary Layer

There are at least four definitions for estimating PBL height: Flux methods, Contour method, Gradient Method and a comparison of these methods (Zullivan, 1998)^[20]. Vertical profiles of potential temperature, provides a first order approach of structure of mixed and stable boundary layer (SBL). When the surface is cooler than air, the atmosphere forms a stable stratified layer; under radiative forcing, there is a strong diurnal variation in near-ground air temperature, and the amplitude of variation decreases with height. Most of solar radiation is absorbed by the ground, which then transfers the heat to the air via surface heat fluxes. The heat is further transported up via turbulence eddies. The magnitude of vertical temperature gradient in the daytime capping inversion is important because it is a measure of the rate of vertical diffusion, through the capping inversion.

There are at least four definitions for estimating PBL height: Flux methods, Contour method, Gradient Method and a comparison of these methods (Zullivan, 1998)^[20]. Vertical profiles of potential temperature, provides a first order approach of structure of mixed and stable boundary layer (SBL). Under radiative forcing, there is a strong diurnal variation in near-ground air temperature, and the amplitude of variation decreases with height. Most of solar radiation is absorbed by the ground, which then transfers the heat to the air via surface heat fluxes. The heat is further transported up via turbulence eddies. The magnitude of vertical temperature gradients in the daytime capping inversion is important because it is a measure of the rate of vertical diffusion, through the capping inversion. A criterion to estimate the well mixed layer is the estimation of the Richardson number, defined as:

$$R_i = \frac{\frac{g}{\theta_v} \frac{\partial \theta_v}{\partial z}}{\left[\left(\frac{\partial \bar{U}}{\partial z} \right)^2 + \left(\frac{\partial \bar{V}}{\partial z} \right)^2 \right]^{1/2}} \quad (6.2)$$

Where θ_v is the potential temperature, g is the gravity, \bar{U} and \bar{V} are the components of the horizontal velocity and the vertical space variable. The virtual potential temperature (that determines buoyancy) is nearly adiabatic (i.e., constant with height) in the middle portion of the mixed layer (ML), and is super-adiabatic in the surface layer. At the top of the ML there is usually a stable layer to stop the turbulent

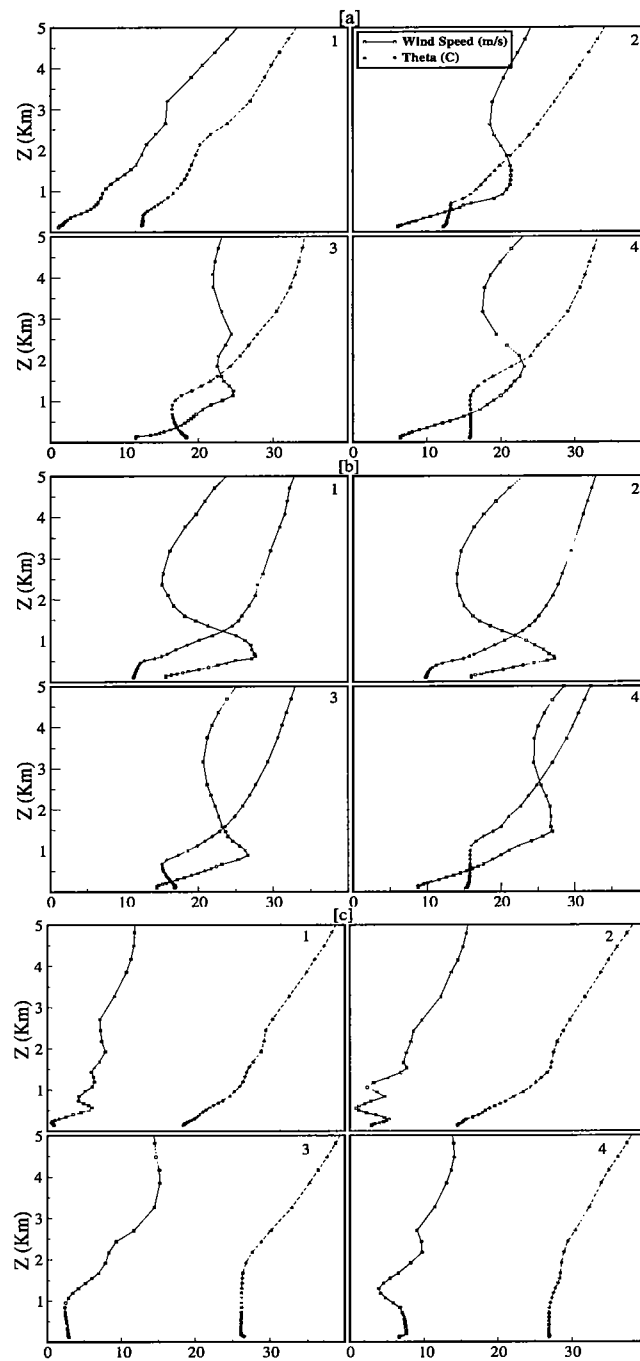


Fig. 6.7: Vertical profiles of 3 days: 24Jan04(a), 25Jan04(b) and a typical 19May03(c). Each 6 hours: 00 LTC(1), 06 LTC(2), 12 LTC(3) and 18 LTC(4)

eddies from rising further. When the layer is very stable so that the temperature increases with height, it is usually called capping inversion. This capping inversion can keep deep convection from developing^[19]. Higher in the SBL, synoptic and mesoscale forcings become important, the wind is usually, increasing with height, reaching maximum at the top of stable layer.

Figure 6.8 shows the simulated time evolution of mixing layer height for two cases: January 23-25 (a) and May 18-20 (b). In both cases, a diurnal oscillation can be distinguished clearly. For the January case, a maximum ML height reaches 1800 mt at the time interval 13-14 LTC, but for other two simulated days this height is clearly lower. For the simulated summer like event in May, the value of the ML height is close to 3.5 Km, for the other two days, the ML height reaches a value of about 2.5 Km. These high values can be explained by the extreme radiative forcing over the ground surface on that day, which produced extreme convective turbulence.

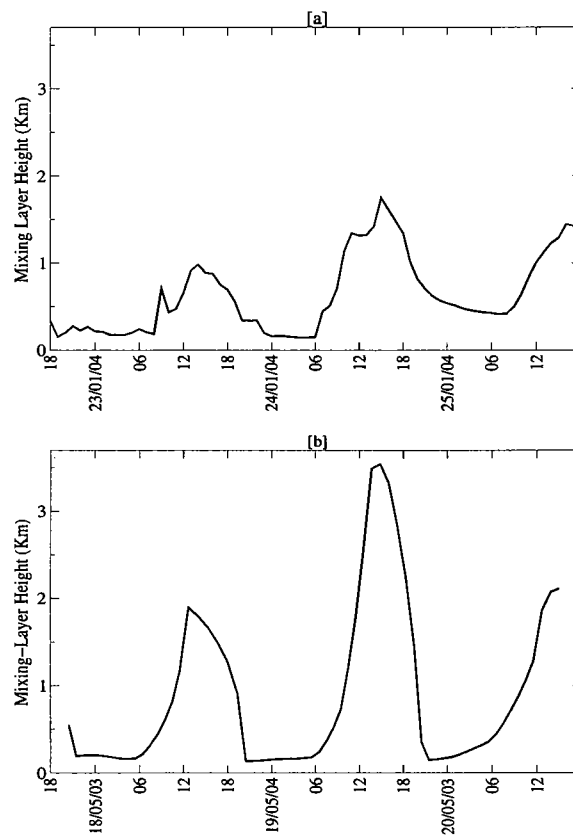


Fig. 6.8: Simulated mixing-layer heights for two cases: Jan04(a) and May03(b)

During the night in both simulations, the values of the ML height are about 250 m above the ground. This order of magnitude of the ML height has been previously reported in many regions^[20, 9, 21]. However, a nocturnal planetary boundary layer, stable straits with small wind speed and cloudlessness is a scheme not well characterized. Local characteristics, such as orography play a determinant role^[20]. However, on January 25 over night, the height of ML increased, compared to the night before, reaching values close

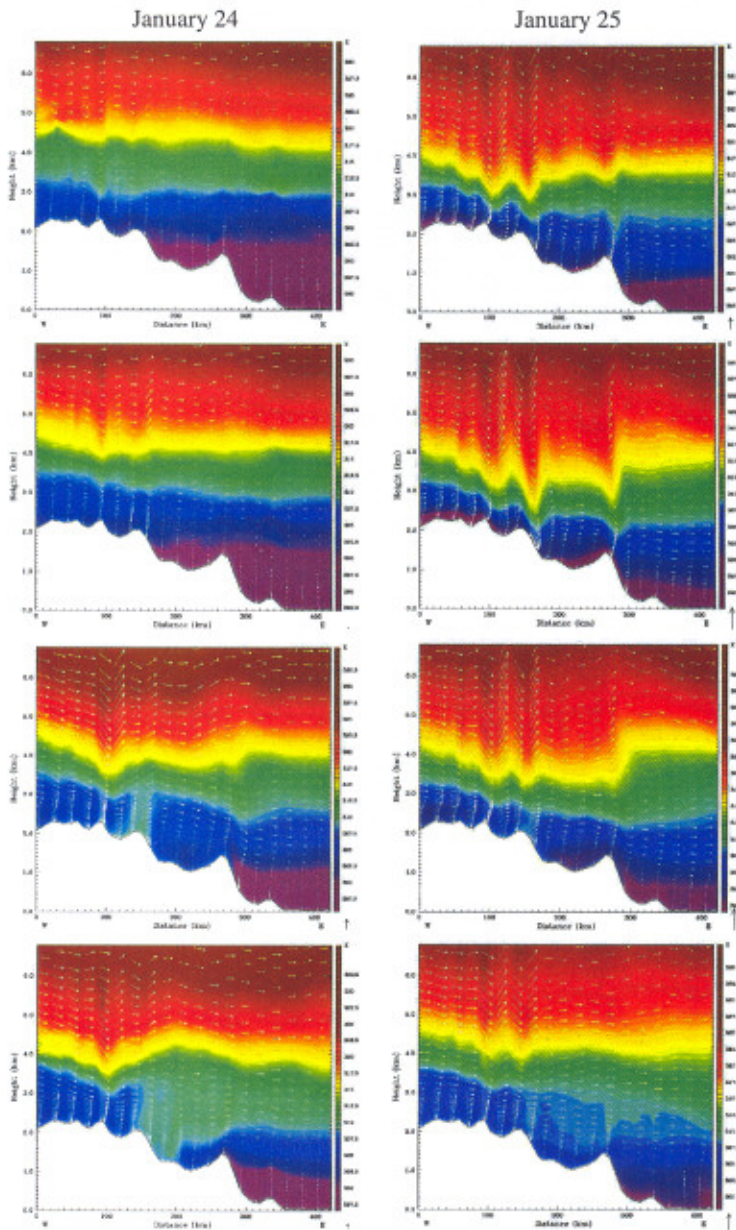


Fig. 6.9: Vertical profile of temperature and wind speed vectors for domain 2

to 600 m. This period occurs indeed, when a strong wind speed appears on the surface between 18 LTC of January 24 and 06 LT of day 25. This behavior may be due to the presence of advective turbulence and Low-level jet presence. This can be explained by the evolution of the intensity of winds in this region. In figure a series of plots along a transect joining the highland region on west side and the low Huasteca region on the east. It can be seen that a kind of Low Level Jet develops.

Some waves can modify the SBL to the point where periods of static instability occur, leading to bursts

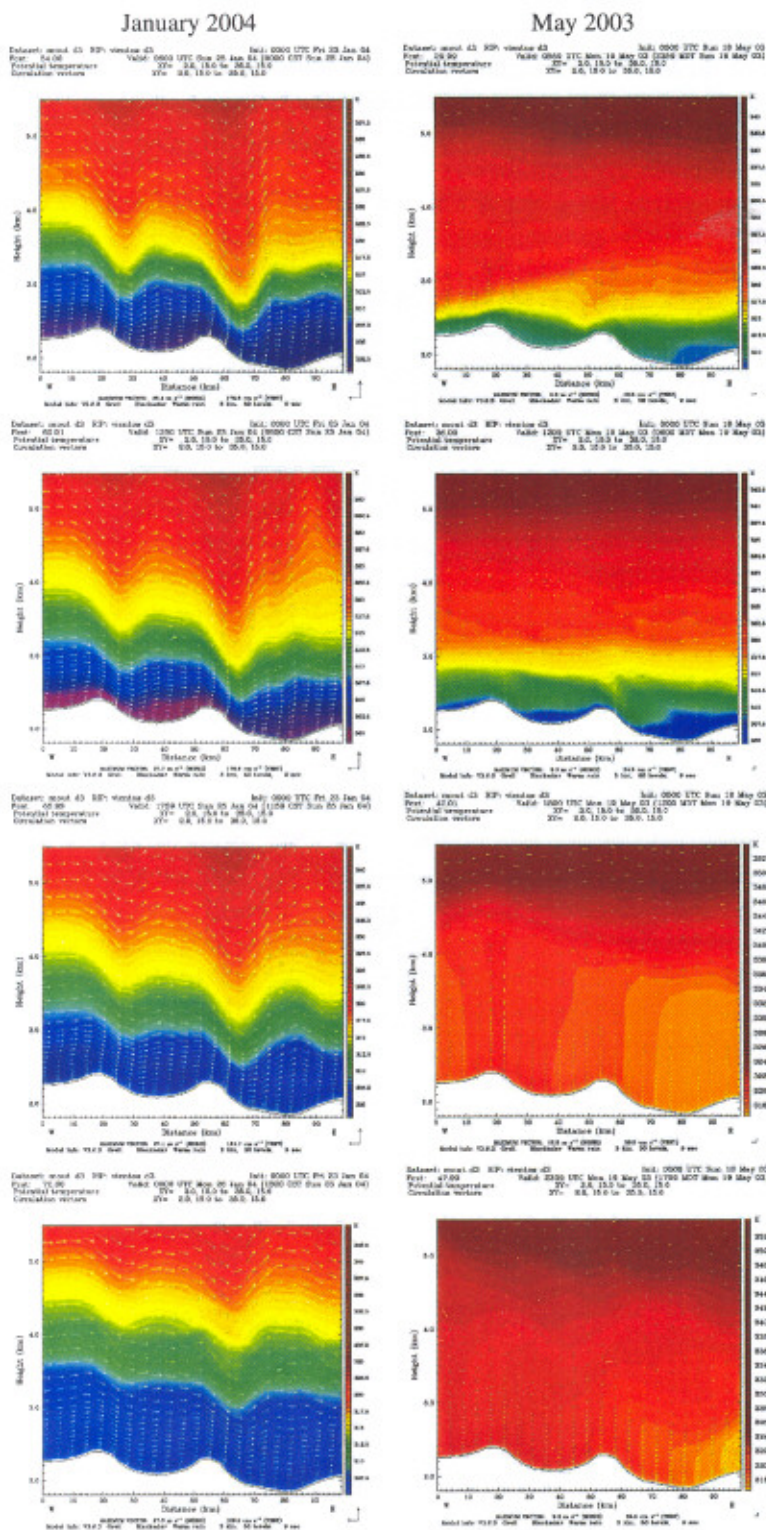


Fig. 6.10: Vertical profile of temperature and wind speed vectors for domain 3

of convective turbulence during portions of the wave cycle. Stability suppresses and instability enhances vertical turbulent motions. In a stable stratification buoyancy oscillations may occur as **gravity waves**^[19]. Gravity wave activity can serve as the transport mechanism for extreme winds, and Brauser concludes that the turbulent structure is of prime importance^[6].

Figure 6.9 shows a cross section along the domain two on 00 LTC on January 25. The principal mountains, hills and valleys can be distinguished. Three different region can be differentiated (1) The valley of SLP, (2) the Rioverde valley and (3) Huasteca; all of them previously described before. This is a contour plot where potential temperature gradient and wind speed vectors can be seen.

A temperature gradient and a stratified layer 1 Km above the surface are clearly seen. In this layer, strong oscillations take place that correspond with the local orography. In addition, we see that the high value of the wind speed vectors on the surface contrast with the wind vector associated with the oscillations. Reference 1 is clearly divergent over the valley and convergent downhill on the right side of reference 1; and the convergent vectors are above reference 2, and divergent on the right of the same reference, there are no high values of wind speed in region 3.

These waves were reported beforehand: Finningan, *et al.* (1984) observed dramatic sequences of large amplitude waves and computed these levels at 550 and 650^[9]. On the other hand lee waves may have formed downstream and contributed to acceleration of the flow on upwind slopes in the Valleys on the other side. However, all references link gravity waves present after sunset, but here these structures appear at midnight.

6.4.3 Katabatic winds

In absence of well characterized synoptic and mesoscale forcings, local factors such as terrain play an important role over meteorological situations on a local grid point. The air near the surface cools because of irradiation forces and high-density air travels downhill in gravity flows, called drainage winds, slope, flows or katabatic winds. The large increases in wind speed are seen because slope irradiance has a greater influence in other areas of the domain. Figure 6.11 shows surface temperature and wind speed vectors of 2 day simulations, at 4 time steps: 00, 06, 12 and 18 LTC. The figure shows a horizontal wind speed increase on 00 LT of January 25.

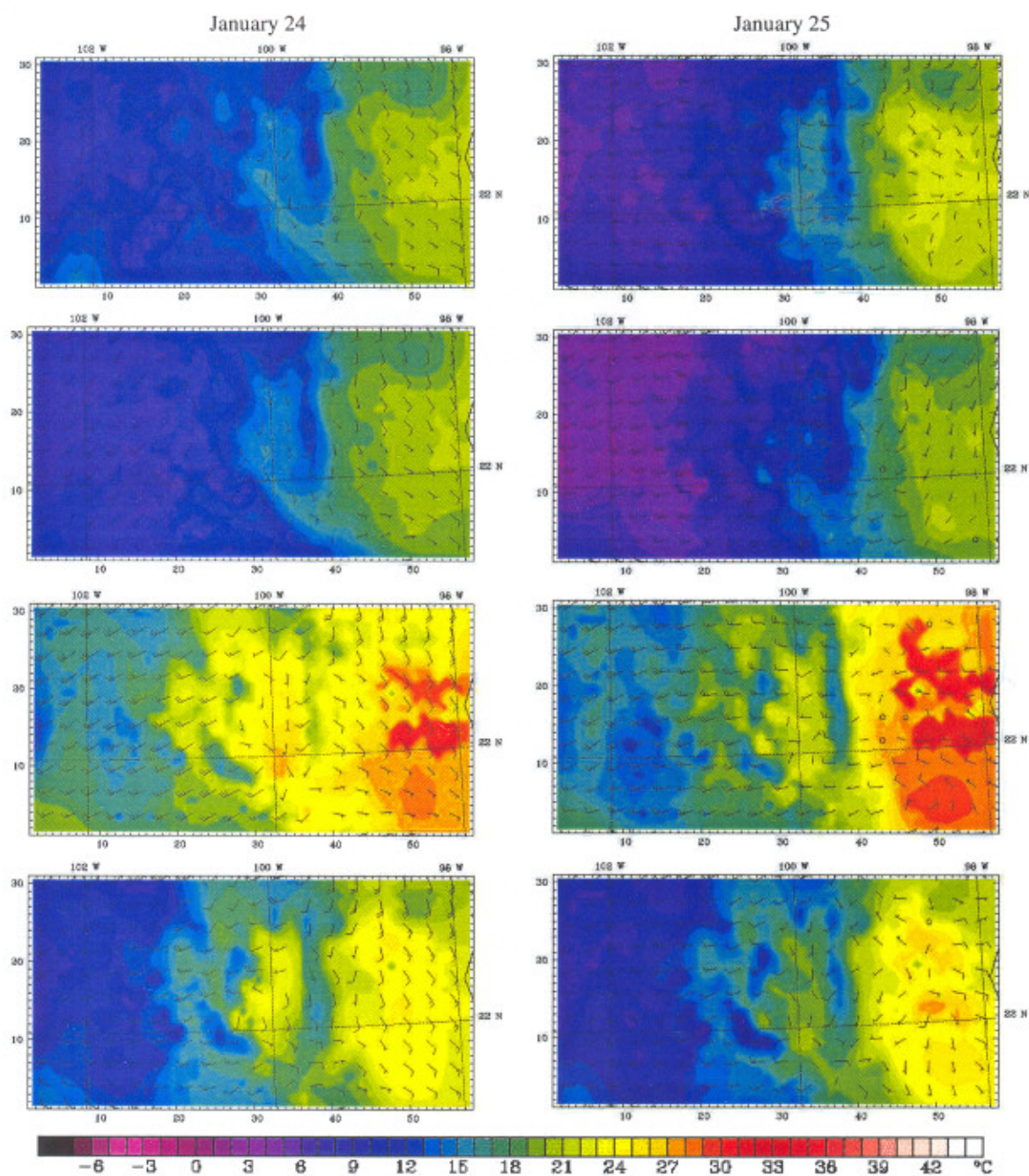


Fig. 6.11: Surface temperature and wind vectors for two days and 4 simulated hours for top to bottom: 00,06,12 and 18 LTC respectively

7

Conclusions and future recommendations

The mesoscale numerical model MM5, developed by the Penn State University and NCAR, U.S.A, was adapted to simulate the atmosphere circulation in the San Luis Potosi, Valley, Mexico. Two principal numerical experiments were carried out:

- a) The simulation of strong wind events, which occur frequently in the January and February months every year. These atmospheric phenomena are closely connected with the synoptic situation which results from the movement of cold fronts southwards. The results of the general circulation of the studied area favours strongly the generation of intense wind speeds over the central-north part of Mexico.
- b) To contrast the above mentioned outstanding events, a typical warm summer situation was also modelled. Since in the San Luis Potosi Valley, the highest monthly mean temperature takes place in May, the atmospheric circulation was simulated for May 18th, 19th and 20th of 2003.

Three principal outcomes of these numerical simulations were found:

1. The manifestation of the strong wind event in the January simulation reflects the presence of a Low Level Jet. The results reveal how this LLJ interacts with the complex orography and where the major intensities occur.
2. The interaction of this strong wind event with the orography shows clearly the generation of gravity waves.
3. As a result of the differential effect of solar radiation and of the valley mountains orography in the San Luis Potosi Valley, a Katabatic wind system could be distinguished in some areas of the modelled region.

Although there is a lack of information on measured meteorological parameters in the considered domain, it was possible to compare the outcomes of the model with observed data at two meteorological stations. The comparison between calculated and observed data of temperature, wind speed and direction reveal a good agreement, which is of the same order of magnitude as those reported in the literature. Furthermore, the observed evolution of clouds during the wind event is reproduced very well by the model through the vertically integrated water column.

Conclusions and future recomendations

The adaptation of the model to the San Luis Potosi valley will allow elaborating futher research work like the transport of contaminants and aerolsols. To improve the inputs in to the model of physical parameter like soil moisture, albedo, land use, etc. is necessary to carry out intensive observations (rawinsondes, heat exchages, etc...) in the diferent climate zones of the consider domain.

Bibliography

- [1] Beniston , M., *From Turbulence to Climate*, Springer, Berlin, Germany, 1998, ISBN 3-540-63495-9.
- [2] Brausser, O., 2001: Development and Application of a Physical Approach to Estimate Wind Gust, *Monthly Weather Review*, **129**, 5-25.
- [3] Chen, F., and Dudhia J., 2001: Couplin an Advanced Land Surface-Hydrology Model with the Penn State-NCAR MM5 Modeling System. Part I:Model Implementation and Sensitivity , *Mont. Wea. Rew.* **129** 569-585
- [4] Chen, F., and Dudhia J., 2001: Couplin an Advanced Land Surface-Hydrology Model with the Penn State-NCAR MM5 Modeling System. Part I:Model Implementation and Sensitivity , *Mont. Wea. Rew.* **129** 587-604.
- [5] Chen, F., Manning, K., and Rife, D., 2002: Evaluating the Performance of the MM5OSULSM Realtime Forecast System for Semi-Arid and Desert Areas, Twelfth PSUNCAR Mesoscale Model Users' Workshop.
- [6] Dailey, P.S., and Keller, J.L. 2002: Modeling of Extreme Wind Events Using MM5: Approach and Verification, Twelfth PSUNCAR Mesoscale Model Users' Workshop.
- [7] Dudhia, J., 1993: A nonhydrostatic version of the Penn State-NCAR Mesoscale Model: Validation test and simulations of an Atlantic cyclone and cold front, *Mont. Wea. Rew.* **121**, 1493-1513.
- [8] Dudhia, J., and Bresch, J.F., 2003: Verification of the Global Version of MM5. Thirteenth PSUNCAR Mesoscale Model Users' Workshop
- [9] Goyette, S., Breinston, M., Caya, D., Laprise, R., and Jungo, P., 2001: Numerical Investigation of an Extreme Storm with the Canadian Regional Climate Model: the case study of windstorm VIVIAN, Switzerland, February 27, 1990, *Climate Dynamics*, **18**, 145-168.
- [10] Grell, G.A., Dudhia, J., and Stauffer, D.R., 1995: A description of the Fifth-Generation Penn StateNCAR Mesoscale Model (MM5), Tech. Rep. NCARTN-398+STR, National Center of Atmospheric Research (NCAR), Bolder (CO), USA

- [11] Hanna, S.R., and Yang, R., 2001: Evaluations of Mesoscale Models Simulations of Near-Surface Winds, Temperature Gradients, and Mixing Depths, *J. Appl. Meteor.* **40**, 1095-1104.
- [12] Hauge, G., 2002: Simulation of surface temperature inversions in complex terrain and implementation of slope irradiance, Twelfth PSUNCAR Mesoscale Model Users' Workshop .
- [13] Instituto Nacional de Estadística, Geografía e Informática (INEGI), 2000: Carta de Uso del Suelo y Vegetación, 1:250 000.
- [14] Otte, T.L., 2001: Using MM5v3 with Eta Analyses for Air-Quality Modeling at the EPA, Eleventh PSUNCAR Mesoscale Model Users' Workshop
- [15] Parish, T.R., and Cassano, J.J., 2003: Diagnosis of the Katabatic Wind Influence on the Wintertime Antarctic Surface Wind Field for Numerical Simulations, *Mont. Wea. Rev.* **131**, 1128-1139.
- [16] Rzedowski, J. 1966: Vegetación del Estado de San Luis Potosí, Contribuciones del Instituto de Investigación en zonas desérticas No. 20, Universidad Autónoma de San Luis Potosí.
- [17] Smith, S.A., 2003: Observations and simulations of the 8 November 1999 MAP Mountain Wave Case, *Q.J.R. Meteorol. Soc.*, **128** 1-999.
- [18] Smith, S.A., and Broad, A.S., 2002: Horizontal and Temporal Variability of Mountain Waves over Mont Blanc, *Q.J.R. Meteorol. Soc.*, **128**, 1-999.
- [19] Stull, R.B., *An Introduction to Boundary Layer Meteorology*, Kluwer Academic Publishers, Dordrecht, The Netherlands, 1997 edn, 1988, ISBN 90-277-2768-6.
- [20] Sullivan, P.P., Moeng, C., Stevens, B., Lenschow, D.H., and Mayor, S.D., 1998: Structure of the Entrainment Zone Capping the Convective Atmospheric Boundary Layer, *J. Atmos. Sci.*, **55**, 3042-3064
- [21] Vellinga, O.S., 2001: Intercomparison of Local and Non-Local Atmospheric Boundary-Layer Schemes in MM5 with Detailed Observations, MSc. Thesis.
- [22] Vilá-Guerau de Arellano, Jordi, 1992: The influence of turbulence on chemical reactions in the atmospheric boundary layer, PhD thesis, IMAU University of Utrecht, The Netherlands.
- [23] Wilson, J.D., and Flesch, T.K. 2003: An Idealized Mean Wind Profile for the Atmospheric Boundary Layer, *Boundary Layer Meteo.*, **110**, 281-299.
- [24] Wisse J.S.P., and Vila-Guerau J., 2004: Analysis of the role of the planetary boundary layer schemes during a several convective storm, *Annales Geophysicae* **22**, 1-14.
- [25] Wurtele, M.G., Datta, A., and Sharman, R.D., 1993: Lee waves: Bening and Malignant, NASA Contractor Report 186024.
- [26] Yamazaki, Y., Manzo, M.D., Martins, V.M., and Pinto, P., 2003: A MM5 Extreme Precipitation Event Forecast Over Portugal Thirteenth PSUNCAR Mesoscale Model Users' Workshop.
- [27] Zhang, D.L., and Zheng, W.Z., 2004: Diurnal Cycles of Surface Winds and Temperatures as Simulated by Five Boundary Layer Parameterizations, *J. Appl. Meteor.* **43**, 150-169.